

Generalized Bayesian Filtering via Sequential Monte Carlo

Ayman Boustati^{1,2}, Ömer Deniz Akyildiz^{1,2}, Theodoros Damoulas^{1,2}, and Adam Johansen^{1,2}

¹The Alan Turing Institute, London

²University of Warwick

Abstract

We introduce a framework for inference in general state-space hidden Markov models (HMMs) under likelihood misspecification. In particular, we leverage the loss-theoretic perspective of generalized Bayesian inference (GBI) to define generalized filtering recursions in HMMs, that can tackle the problem of inference under model misspecification. In doing so, we arrive at principled procedures for robust inference against observation contamination through the β -divergence. Operationalizing the proposed framework is made possible via sequential Monte Carlo methods (SMC). The standard particle methods, and their associated convergence results, are readily generalized to the new setting. We demonstrate our approach to object tracking and Gaussian process regression problems, and observe improved performance over standard filtering algorithms.

1 Introduction

Estimating the hidden states in dynamical systems is a long-standing problem in many fields of science and engineering. It is customary to formulate this problem as an inference problem of a general state-space hidden Markov model (HMM) which is defined via two processes, *the hidden process*, denoted $(\mathbf{x}_t)_{t \geq 0}$, and *the observation process*, denoted $(\mathbf{y}_t)_{t \geq 1}$, respectively. More precisely, we consider the general state-space hidden Markov models of the form

$$\mathbf{x}_0 \sim \pi_0(\mathbf{x}_0), \quad (1)$$

$$\mathbf{x}_t | \mathbf{x}_{t-1} \sim f_t(\mathbf{x}_t | \mathbf{x}_{t-1}), \quad (2)$$

$$\mathbf{y}_t | \mathbf{x}_t \sim g_t(\mathbf{y}_t | \mathbf{x}_t), \quad (3)$$

where $\mathbf{x}_t \in \mathsf{X}$ for $t \geq 0$, $\mathbf{y}_t \in \mathsf{Y}$ for $t \geq 1$, f_t is a Markov kernel on X and $g_t : \mathsf{Y} \times \mathsf{X} \rightarrow \mathbb{R}_+$ is the likelihood function. We assume $\mathsf{X} \subseteq \mathbb{R}^{d_x}$ and $\mathsf{Y} \subseteq \mathbb{R}^{d_y}$ for convenience; the extension to general Polish spaces is direct. A key inference problem for this class of models is constructing (or estimating) the posterior probability distributions of the hidden states $(\mathbf{x}_t)_{t \geq 0}$ given the observations $\mathbf{y}_{1:t}$ which are denoted as $(\pi_t(\mathbf{x}_t | \mathbf{y}_{1:t}))_{t \geq 1}$ and termed as the *filtering distributions*. This task is more generally known as *Bayesian filtering* (Anderson and Moore, 1979, Särkkä, 2013).

Under linear and Gaussian assumptions, the inference problem for the hidden states of HMMs can be solved analytically via the Kalman filter (Kalman, 1960). However, inference for general HMMs of the form (1)–(3) with nonlinear, non-Gaussian transitions and likelihoods lacked a general, principled solution until the arrival of the particle filtering schemes (Gordon et al., 1993). Firstly proposed as simple evolutionary methods, the particle filters (PFs) have become ubiquitous

in Bayesian filtering in the general setting. In short, the PFs retain a weighted collection of Monte Carlo samples representing the filtering distribution $\pi_t(\mathbf{x}_t|\mathbf{y}_{1:t})$ and recursively approximate the sequence of distributions $(\pi_t)_{t \geq 0}$ using a mutation-selection scheme (Doucet et al., 2000).

When performing model based inference, it is important to consider whether the proposed model class includes the true data-generating mechanism (DGM). In particular, for general state-space HMMs, misspecification may happen if the dynamics of the hidden process significantly differ from the assumed model f_t , or if the observations are produced in a way that is markedly different from the assumed likelihood model g_t , e.g. due to corruption by heavier tailed noise. The latter case of likelihood misspecification, is of widespread interest within the field of *robust statistics* (Huber, 2011) and has recently attracted significant interest in the machine learning community (Futami et al., 2018). It is the misspecified likelihood setting that this paper seeks to address.

When one cannot model the true DGM, a principled approach to address model misspecification is to employ a generalized version of Bayesian inference, proposed in Bissiri et al. (2016). This approach views the classical Bayesian inference as a loss minimization procedure in the space of probability measures, a view first developed by Zellner (1988). In particular, the standard Bayesian update can in this view, where one constructs the loss function using the Kullback-Leibler (KL) divergence between the empirical distribution of the observations and the assumed likelihood (Bissiri et al., 2016). The KL divergence is sensitive to outliers (see Knoblauch et al. (2019) for a general discussion), hence the overall Bayesian inference procedure is not robust to observations which are incompatible with the assumed likelihood model. A principled remedy to this problem is replacing the KL divergence with alternative measures, such as the β -divergence, which can make the overall procedure more robust (Cichocki and Amari, 2010) while retaining interpretability.

Robust particle filters have been proposed before, in order to handle outliers, sensor failures and misspecification of the transition model, including (Maiz et al., 2009, 2012, Xu et al., 2013, Calvet et al., 2015, Teixeira et al., 2017, Hu et al., 2007, Akyildiz and Míguez, 2020). These methods are, however, either based on heuristic outlier detection schemes that are problem specific or make strong assumptions about the nature of the DGM in order to justify the use of heavy-tailed distributions (Xu et al., 2013). This requires knowledge of the contamination mechanism that is implicitly embedded in the likelihood.

In this work we propose an alternative principled approach to robust filtering that does not impose unnecessary additional modelling assumptions. We adapt the generalized Bayesian inference (GBI) approach of Bissiri et al. (2016) to the Bayesian filtering setting and show that sequential Monte Carlo (SMC) methods can be used to perform this inference. We illustrate the performance of this approach, using β -divergence to mitigate against the presence of outliers. We show that this approach significantly improves the PF performance in data contamination settings, while retaining a general and principled approach to inference. We provide empirical results that demonstrate improvement over Kalman and particle filters for both linear and non-linear HMMs. Finally, exploiting the state-space representations of Gaussian processes (GPs) (Särkkä et al., 2013), we demonstrate our framework on London air pollution data using robust GP regression which has linear time-complexity in the number of observations.

Notation. We denote the space of bounded, Borel measurable functions on X as $B(X)$. We denote the Dirac measure located at y as $\delta_y(dx)$ and note that $f(y) = \int f(x)\delta_y(dx)$ for $f \in B(X)$. We denote the Borel subsets of X as $\mathcal{B}(X)$ and the set of probability measures on $(X, \mathcal{B}(X))$ as $\mathcal{P}(X)$. For a probability measure $\mu \in \mathcal{P}(X)$ and $\varphi \in B(X)$, we write $\mu(\varphi) := \int \varphi(\mathbf{x})\mu(d\mathbf{x})$. Given a probability measure μ , we often abuse the notation and denote its density with respect to the Lebesgue measure as $\mu(\mathbf{x})$.

2 Background

2.1 Generalized Bayesian Inference

Parametric Bayesian inference implicitly assumes that the generative model is well-specified, in particular, the observations are generated from the assumed likelihood model. In general, this assumption may not hold in real-world scenarios. Hence, one may wish to take into account the discrepancy between the true DGM and the assumed likelihood. Generalized Bayesian inference (GBI) is an approach proposed in [Bissiri et al. \(2016\)](#) to deal with such cases.

For the simple Bayesian updating setup, consider a prior π_0 and the assumed likelihood function $g(\mathbf{y}|\mathbf{x})$. The posterior $\pi(\mathbf{x}|\mathbf{y}) =: \pi(\mathbf{x})$ is given by Bayes rule

$$\pi(\mathbf{x}) = \pi_0(\mathbf{x}) \frac{g(\mathbf{y}|\mathbf{x})}{Z}, \quad (4)$$

where $Z := \int g(\mathbf{y}|\mathbf{x})\pi_0(\mathbf{x})d\mathbf{x}$. [Zellner \(1988\)](#) and [Bissiri et al. \(2016\)](#) showed that (4) can be seen as a special case of a more general update rule, which can be described as a solution of an optimization problem in the space of measures. In particular, let $L(\nu; \pi_0, \mathbf{y})$ be a loss-function where ν is a probability measure and π_0 is the prior, a belief distribution over \mathbf{x} can be constructed by solving

$$\hat{\nu} = \arg \min_{\nu} L(\nu; \pi_0, \mathbf{y}). \quad (5)$$

To obtain Bayes-type updating rules, one needs to specify this loss function as a sum of a “data term” and a “regularization term” ([Bissiri et al., 2016](#)) given as

$$L(\nu; \pi_0, \mathbf{y}) = \lambda_1(\nu, \mathbf{y}) + \lambda_2(\nu, \pi_0), \quad (6)$$

where λ_1 defines a data dependent “loss” and λ_2 controls the discrepancy between the prior and the final belief distribution $\hat{\nu}$. [Bissiri et al. \(2016\)](#) show that the form of (6) that satisfies the von Neumann–Morgenstern utility theorem ([von Neumann and Morgenstern, 1947](#)) and Bayesian additivity¹ is given by

$$L(\nu; \pi_0, \mathbf{y}) = \int \ell(\mathbf{x}, \mathbf{y})\nu(d\mathbf{x}) + \text{KL}(\nu||\pi_0), \quad (7)$$

which leads to a Bayes-type update [Bissiri et al. \(2016\)](#), [Jewson et al. \(2018\)](#), given by

$$\pi(\mathbf{x}) = \pi_0(\mathbf{x}) \frac{G(\mathbf{y}|\mathbf{x})}{Z}, \quad (8)$$

with $G(\mathbf{y}|\mathbf{x}) := \exp(-\ell(\mathbf{x}, \mathbf{y}))$ where $\ell(\mathbf{x}, \mathbf{y})$ is some divergence measuring the discrepancy between the observed information and the assumed model. In particular, if one assumes the real-world likelihood, i.e. the DGM, h_0 , is different from the model likelihood g and defines $\ell(\mathbf{x}, \mathbf{y})$ as a Kullback–Leibler (KL) divergence between the empirical likelihood \tilde{h}_0 (an empirical measure constructed using the observations) and the assumed likelihood $g(\mathbf{y}|\mathbf{x})$, the standard Bayes rule (4) arises as a solution. To see this, we can employ the KL divergence as a loss,

$$\text{KL}(h_0||g) = \int \log h_0(\mathbf{y}')h_0(d\mathbf{y}') - \int \log g(\mathbf{y}'|\mathbf{x})h_0(d\mathbf{y}'),$$

¹Bayesian additivity, also referred to as coherence says that applying a sequence of updates with subsets of the data should give rise to the same posterior distribution as single update employing all of the data.

and note that the first term does not affect the solution of optimization problem (5). Hence we arrive at the integrated loss function

$$\tilde{\ell}(\mathbf{x}) = - \int \log g(\mathbf{y}'|\mathbf{x}) h_0(d\mathbf{y}'). \quad (9)$$

By replacing the true likelihood h_0 with its empirical approximation upon observing \mathbf{y} , i.e., setting $h_0(d\mathbf{y}') \approx \delta_{\mathbf{y}}(d\mathbf{y}')$, we obtain $\tilde{\ell}(\mathbf{x}) \approx \ell(\mathbf{x}, \mathbf{y}) = -\log g(\mathbf{y}|\mathbf{x})$, which can be plugged in to (8) resulting in the standard Bayes update (4).

As previously mentioned, due to the properties of the KL divergence, the standard Bayes update is not robust to outliers (Knoblauch et al., 2019). Hence, substituting the KL with a more robust divergence such as the β -divergence, can endow inference with more robustness. Specifically, if ℓ is chosen as a β -divergence, the one step Bayes update for the likelihood $g(\mathbf{y}|\mathbf{x})$ can be written as

$$\pi(\mathbf{x}) = \pi_0(\mathbf{x}) \frac{G^\beta(\mathbf{y}|\mathbf{x})}{Z_\beta}, \quad (10)$$

where

$$G^\beta(\mathbf{y}|\mathbf{x}) = \exp\left(\frac{1}{\beta} g(\mathbf{y}|\mathbf{x})^\beta - \frac{1}{\beta+1} \int g(\mathbf{y}'|\mathbf{x})^{\beta+1} d\mathbf{y}'\right). \quad (11)$$

One can then see $G^\beta(\mathbf{y}|\mathbf{x})$ as a generalized likelihood, resulting from the use of a different loss function compared to the standard Bayes procedure. Here β is a hyperparameter that needs to be selected depending on the degree of misspecification. In general $\beta \in (0, 1)$ and

$$\lim_{\beta \rightarrow 0} G^\beta(\mathbf{y}|\mathbf{x}) = g(\mathbf{y}|\mathbf{x}). \quad (12)$$

Thus, intuitively, small β values are suitable for mild model misspecification and large β values are suitable when the assumed model is expected to significantly deviate from the true model. In the experimental section, we devote some attention to the selection of β and sensitivity analysis.

Generalised Bayesian updating in the form (10) is more robust against outliers if a suitable divergence is chosen Ghosh and Basu (2016), Knoblauch et al. (2018, 2019). Later, we will demonstrate how this approach can be used to construct robust particle filtering procedures.

2.2 Sequential Monte Carlo for HMMs

Let $\mathbf{x}_{1:T}$ be a hidden process with $\mathbf{x}_t \in \mathbf{X}$ and $\mathbf{y}_{1:T}$ an observation process with $\mathbf{y}_t \in \mathbf{Y}$. Recall that we are interested in conducting inference in HMMs of the form (1)–(3) where $\pi_0(\cdot)$ is a prior probability distribution on the initial state \mathbf{x}_0 , $f_t(\mathbf{x}|\mathbf{x}')$ is a Markov transition kernel on \mathbf{X} and $g_t(\mathbf{y}_t|\mathbf{x}_t)$ is the likelihood for observation \mathbf{y}_t . We assume that the observation sequence $\mathbf{y}_{1:T}$ is fixed but otherwise arbitrary.

The typical interest in probabilistic models is the estimation of expectations of general test functions with respect to the posterior distribution, in this case, of the hidden process $\pi_t(\mathbf{x}_t|\mathbf{y}_{1:t})$ and the joint distributions $\mathbf{p}_t(\mathbf{x}_{0:t}|\mathbf{y}_{1:t})$. More precisely, given a bounded test function $\varphi \in B(\mathbf{X})$, we are interested in estimating integrals of the form

$$\pi_t(\varphi) = \int \varphi(\mathbf{x}_t) \pi_t(\mathbf{x}_t|\mathbf{y}_{1:t}). \quad (13)$$

When the transition kernels f_t and the likelihoods g_t are linear-Gaussian, the distributions $(\pi_t, \mathbf{p}_t)_{t \geq 0}$ can be found in closed form with the Kalman filter (Kalman, 1960, Anderson and

Moore, 1979). However, when the Markov kernels f_t and the likelihood functions g_t are non-linear or non-Gaussian (or both), the distributions of interest are almost always intractable, requiring an alternative approach. One such approach is Sequential Monte Carlo (SMC) methods (Doucet et al., 2000), which are also known as Particle Filters (PFs) when employed in the general state-space HMM setting. PF methods combine importance sampling and resampling within algorithms tailored to the approximate solution of the filtering and smoothing problems, see, e.g., (Doucet et al., 2000, Doucet and Johansen, 2011).

In a typical iteration, a PF method proceeds as follows: given a collection of samples $\{\mathbf{x}_{t-1}^{(i)}\}_{i=1}^N$ representing the posterior $\pi_{t-1}(\mathbf{x}_{t-1}|\mathbf{y}_{1:t-1})$, a PF algorithm first samples from a (possibly observation dependent) proposal

$$\bar{\mathbf{x}}_t^{(i)} \sim q_t(\mathbf{x}_t|\mathbf{x}_{1:t-1}^{(i)}, \mathbf{y}_{1:t}). \quad (14)$$

The algorithm then computes weights for each sample (particle) $\bar{\mathbf{x}}_{t-1}^{(i)}$ in the collection for a given observation \mathbf{y}_t , evaluating its fitness with respect to the likelihood g_t as

$$w_t^{(i)} \propto g_t(\mathbf{y}_t|\bar{\mathbf{x}}_t^{(i)}) \frac{f_t(\bar{\mathbf{x}}_t^{(i)}|\mathbf{x}_{t-1}^{(i)})}{q_t(\bar{\mathbf{x}}_t^{(i)}|\mathbf{x}_{1:t-1}^{(i)}, \mathbf{y}_t)}, \quad (15)$$

where $\sum_{i=1}^N w_t^{(i)} = 1$. Finally, an optional resampling step² is used to prevent particle degeneracy, leading to

$$\mathbf{x}_t^{(i)} \sim \sum_{i=1}^N w_t^{(i)} \delta_{\bar{\mathbf{x}}_t^{(i)}}(d\mathbf{x}_t). \quad (16)$$

One can then construct the empirical probability measure

$$\pi_t^N(d\mathbf{x}_t|\mathbf{y}_{1:t}) = \frac{1}{N} \sum_{i=1}^N \delta_{\mathbf{x}_t^{(i)}}(d\mathbf{x}_t),$$

and the estimate of $\pi_t(\varphi)$ in (13) is given by

$$\pi_t^N(\varphi) = \frac{1}{N} \sum_{i=1}^N \varphi(\mathbf{x}_t^{(i)}). \quad (17)$$

If the proposal is chosen as the transition density, i.e., $q_t(\mathbf{x}_t|\mathbf{x}_{1:t-1}^{(i)}, \mathbf{y}_t) = f_t(\mathbf{x}_t|\mathbf{x}_{t-1}^{(i)})$, we obtain the bootstrap particle filter (BPF) Gordon et al. (1993). This corresponds to the simple procedure of sampling $\bar{\mathbf{x}}_t^{(i)}$ from $f_t(\mathbf{x}_t|\mathbf{x}_{t-1}^{(i)})$, and setting its weight $w_t^{(i)} \propto g_t(\bar{\mathbf{x}}_t^{(i)})$.

3 Generalized Bayesian filtering

In this section, we describe generalized Bayesian filtering recursions. These recursions can be used to perform online generalized Bayesian inference in the HMM setting.

As explained in Section 2.1, given a standard probability model comprised of the prior $\pi_0(\mathbf{x})$ and a likelihood $g(\mathbf{y}|\mathbf{x})$, the general Bayes update defines an alternative, generalized likelihood

²In the simplest form, drawing N times with replacement from the weighted empirical measure to obtain an unweighted sample whose empirical distribution approximates the same target; see Gerber et al. (2019) for an overview of resampling schemes and their properties.

Algorithm 1 The generalized particle filter

Input: Observation sequence $\mathbf{y}_{1:T}$, number of samples N , proposal distributions $q_{1:T}(\cdot)$.

Initialize: Sample $\{\bar{\mathbf{x}}_0^{(i)}\}_{i=1}^N$ for the prior $\pi_0(\mathbf{x}_0)$.

for $t = 1$ **to** T **do**

Sample, for $i = 1, \dots, N$:

$$\bar{\mathbf{x}}_t^{(i)} \sim q_t(\mathbf{x}_t | \mathbf{x}_{1:t-1}^{(i)}, \mathbf{y}_t).$$

Weight, for $i = 1, \dots, N$:

$$w_t^{(i)} \propto \exp(-\ell(\bar{\mathbf{x}}_t^{(i)}, \mathbf{y}_t)) \frac{f_t(\bar{\mathbf{x}}_t^{(i)} | \mathbf{x}_{t-1}^{(i)})}{q_t(\bar{\mathbf{x}}_t^{(i)} | \mathbf{x}_{1:t-1}^{(i)}, \mathbf{y}_t)}.$$

Resample, for $i = 1, \dots, N$,

$$\mathbf{x}_t^{(i)} \sim \sum_{i=1}^N w_t^{(i)} \delta_{\bar{\mathbf{x}}_t^{(i)}}(d\mathbf{x}_t), \quad \text{for } i = 1, \dots, N.$$

end for

$G(\mathbf{y}|\mathbf{x})$. The sequence of generalized likelihoods, denoted as $G_t(\mathbf{y}_t|\mathbf{x}_t)$ for $t \geq 1$, in an HMM yields a joint generalized posterior density which factorizes as

$$p_t(\mathbf{x}_{0:t}|\mathbf{y}_{1:t}) \propto \pi_0(\mathbf{x}_0) \prod_{k=1}^t f_k(\mathbf{x}_k|\mathbf{x}_{k-1}) G_k(\mathbf{y}_k|\mathbf{x}_k), \quad (18)$$

where $G_t(\mathbf{y}_t|\mathbf{x}_t) := \exp(-\ell_t(\mathbf{x}_t, \mathbf{y}_t))$. The inference can be done generically via SMC methods applied to this sequence of twisted probabilities which define a Feynman-Kac flow in the terminology of [Del Moral \(2004\)](#). Next, we present a generalized particle filter via this construction, and describe the special case of the β -bootstrap particle filter (β -BPF), a simple instantiation of the proposed general class of PFs.

3.1 A generalized particle filter

A comparison of the update rules in (4) and (8) suggests a simple generalization of the particle filter. In particular, under the model given by (1)–(3), one can perform generalized inference using $(f_t)_{t \geq 1}$ as usual, but replacing the likelihood with $(G_t)_{t \geq 1}$. Hence, a generalized PF procedure keeps the sampling step intact, but applies a different weight computation step,

$$w_t^{(i)} \propto \exp(-\ell(\bar{\mathbf{x}}_t^{(i)}, \mathbf{y}_t)) \frac{f_t(\bar{\mathbf{x}}_t^{(i)} | \mathbf{x}_{t-1}^{(i)})}{q_t(\bar{\mathbf{x}}_t^{(i)} | \mathbf{x}_{1:t-1}^{(i)}, \mathbf{y}_t)}.$$

The full generalized PF procedure is given in [Algorithm 1](#).

3.2 The β -BPF

In this section, we describe β -BPF which is based on the selection of $\ell_t(\mathbf{x}_t, \mathbf{y}_t)$ as the β -divergence and applying the BPF procedure with the associated generalized likelihood. In this case, the loss is given by

$$\ell_t^\beta(\mathbf{x}_t, \mathbf{y}_t) = \frac{1}{\beta + 1} \int g_t(\mathbf{y}'_t | \mathbf{x}_t)^{\beta+1} d\mathbf{y}'_t - \frac{1}{\beta} g_t(\mathbf{y}_t | \mathbf{x}_t)^\beta. \quad (19)$$

We can then construct the general β -likelihood as³

$$G_t^\beta(\mathbf{y}_t|\mathbf{x}_t) \propto \exp(-\ell_t^\beta(\mathbf{x}_t, \mathbf{y}_t)). \quad (20)$$

In this instance, the use of the β -divergence provides the sampler with robust properties (Cichocki and Amari, 2010). This can informally be seen from the form of the loss function in (19), where for small values of β the exponent tempers the likelihood extending its tails making the loss more forgiving to outliers. The β -BPF procedure is given in Algorithm 2 in the appendix.

Finally, we denote the generalized filters and generalized posteriors for the HMM in the β -divergence setting as π_t^β and p_t^β respectively. Consequently, corresponding quantities constructed by the β -BPF are denoted as $\pi_t^{\beta,N}$ and $p_t^{\beta,N}$.

3.3 Selecting β

It is often the case that the primary goal of inference, particularly in the presence of model misspecification, is prediction. Hence, we propose choosing divergence parameters that lead to maximally predictive posterior belief distributions. In particular, for the β -BPF, define $\mathcal{L}_\beta(\mathbf{y}_t, \hat{\mathbf{y}}_t)$ as a loss function of the observations \mathbf{y}_t and the predictions $\hat{\mathbf{y}}_t$. We propose to choose β as the solution to the following decision theoretic optimisation problem:

$$\min_{\beta} \text{agg}_{t=1}^T (\mathbb{E}_{p(\hat{\mathbf{y}}_t|\mathbf{y}_{1:t-1})} \mathcal{L}_\beta(\mathbf{y}_t, \hat{\mathbf{y}}_t)), \quad (21)$$

where agg denotes an aggregating function. This approach requires some training data to allow the selection of β ; in filtering contexts this can be historical data from the same setting or other available proxies. For offline inference one could also employ the actual data within this framework.

This proposal relies on the quality of the observations, which in the case of outlier contamination is violated by definition. To remedy this, we propose choosing robust versions for agg and \mathcal{L} , e.g. the median and the (standardized) absolute error respectively.

4 Theoretical guarantees

Theoretical guarantees for SMC methods can be extended to the generalized Bayesian filtering setting. Since the generalized Bayesian filters can be seen as a standard SMC methods with modified likelihoods, the same analytical tools can be used in this setting. We provide guarantees for the β -BPF but emphasise that the same results can be obtained much more broadly.

Although the generalized likelihoods $G_t^\beta(\mathbf{y}_t|\mathbf{x}_t)$ are not normalized, they can be considered as potential functions (Del Moral, 2004). Since $G_t^\beta(\mathbf{y}_t|\mathbf{x}_t) < \infty$ whenever $g_t(\mathbf{y}_t|\mathbf{x}_t) < \infty$ and β is fixed, we can adapt the standard convergence results into the generalized case.

Assumption 1. Fix an arbitrary observation sequence $\mathbf{y}_{1:T} \in \mathcal{Y}^{\otimes T}$. The potential functions $(G_t^\beta)_{t \geq 1}$ are bounded and

$$G_t^\beta(\mathbf{y}_t|\mathbf{x}_t) > 0 \quad \forall t \in \{1, \dots, T\}, \mathbf{x}_t \in \mathcal{X}.$$

³Note that the integral term in the divergence expression is independent of \mathbf{x}_t and can be absorbed, without evaluation, into the normalizing constant when \mathbf{x}_t is a location parameter for g_t and \mathcal{Y} is a (linear subspace of) \mathbb{R}^{d_y} . More generally, if g_t is a member of the standard exponential family the integral can be computed by identifying g_t^β with the kernel of another member of the same family with canonical parameters scaled by β . Outside this setting, techniques such as the generalised Poisson estimator Beskos et al. (2006) could be adopted within a random weight particle filter framework Fearnhead et al. (2008).

This assumption holds for most used likelihood functions and their generalized extensions.

Theorem 1. For any $\varphi \in B(\mathcal{X})$, and $p \geq 1$,

$$\|\pi_t^{\beta,N}(\varphi) - \pi_t^\beta(\varphi)\|_p \leq \frac{c_{t,p,\beta} \|\varphi\|_\infty}{\sqrt{N}}, \quad (22)$$

where $c_{t,p,\beta} < \infty$ is a constant independent of N .

The proof sketch and the constant $c_{t,p,\beta}$ can be found in the supplement. This L_p bound provides a theoretical guarantee on the convergence of particle approximations to generalized posteriors. The special case when $p = 2$ also provides the error bound for the mean-squared error. It is well known that Theorem 1 with $p > 2$ leads to a law of large numbers via Markov's inequality and a Borel-Cantelli argument:

Corollary 1. Under the setting of Theorem 1, we have

$$\lim_{N \rightarrow \infty} \pi_t^{\beta,N}(\varphi) = \pi_t^\beta(\varphi) \quad \text{a.s.} \quad \text{for } t \geq 1. \quad (23)$$

Finally, a central limit theorem for estimates of expectations with respect to the smoothing distributions can be obtained by considering the path space $\mathcal{X}^{\otimes t}$. Recall the joint posterior $p_t^\beta(\mathbf{x}_{1:t}|\mathbf{y}_{1:t})$ and consider a test function $\varphi_t : \mathcal{X}^{\otimes t} \rightarrow \mathbb{R}$. We denote $\bar{\varphi}_t^\beta := \int \varphi_t^\beta(\mathbf{x}_{1:t}) p_t^\beta(\mathbf{x}_{1:t}|\mathbf{y}_{1:t})$ and denote the β -BPF estimate of $\bar{\varphi}_t$ with

$$\bar{\varphi}_t^{\beta,N} := \int \varphi_t(\mathbf{x}_{1:t}) p_t^{\beta,N}(\mathbf{x}_{1:t}).$$

Theorem 2. Under the regularity conditions given in [Chopin \(2004, Theorem 1\)](#), we have

$$\sqrt{N} \left(\bar{\varphi}_t^{\beta,N} - \bar{\varphi}_t^\beta \right) \xrightarrow{d} \mathcal{N} \left(0, \sigma_{t,\beta}^2(\varphi_t) \right), \quad (24)$$

as $N \rightarrow \infty$ where $\sigma_{t,\beta}^2(\varphi_t) < \infty$.

The expression $\sigma_{t,\beta}^2(\varphi_t)$ can be found in the appendix. These results illustrate that the standard guarantees for generic particle filtering methods extend to our case.

5 Experiments

In this section, we illustrate the properties of the β -BPF and empirically verify its robustness.

Throughout this section, we report the *normalised mean squared error (NMSE)* and the *90% empirical coverage* as goodness-of-fit measures. The NMSE scores indicate the mean fit for the inferred posterior distribution and the empirical coverage measures the quality of its uncertainty quantification. We further note that any claim in performance difference is based on the Wilcoxon signed-rank test. We give further in-depth details on the experimental setup and further results in the supplementary material.

5.1 A Linear-Gaussian state-space model

The Wiener velocity model ([Särkkä and Solin, 2019](#)) is a standard model found in the target tracking literature, where the velocity of a particle is modelled as a Wiener process. The

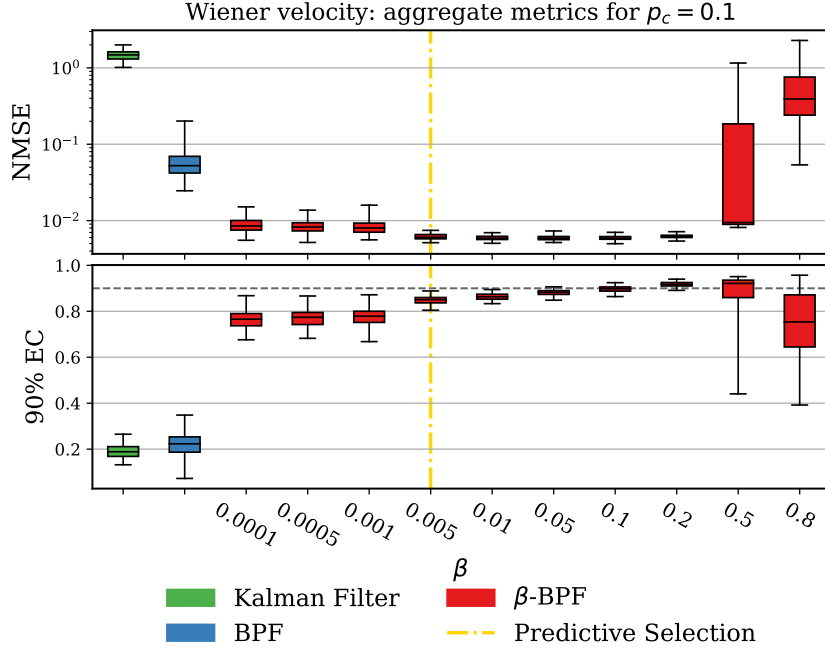


Figure 1: The mean metrics over state dimensions for the Wiener velocity example with $p_c = 0.1$. The top panel presents the NMSE results (lower is better) and the bottom panel presents the 90% empirical coverage results (higher is better), on 100 runs. The vertical dashed line in gold indicate the value of β chosen by the selection criterion in Section 3.3. The horizontal dashed line in black in the lower panel indicates the 90% mark for the coverage.

discretized version of this model can be represented as a Linear-Gaussian State-Space model (LGSSM),

$$\mathbf{x}_t = \mathbf{A}\mathbf{x}_{t-1} + \boldsymbol{\nu}_{t-1}, \quad \boldsymbol{\nu}_t \sim \mathcal{N}(\mathbf{0}, \mathbf{Q}) \quad (25)$$

$$\mathbf{y}_t = \mathbf{H}\mathbf{x}_t + \boldsymbol{\epsilon}_t, \quad \boldsymbol{\epsilon}_t \sim \mathcal{N}(\mathbf{0}, \boldsymbol{\Sigma}) \quad (26)$$

where \mathbf{A} , \mathbf{Q} are state-transition parameters dictated by the continuous-time model and \mathbf{H} is the observation matrix (see Appendix). We simulate this model in two-dimensions with $\boldsymbol{\Sigma} = \mathbf{I}$, contaminating the observations with a large scale, zero-mean Gaussian, $\mathcal{N}(0, 100^2)$ with probability p_c . Our aim is to obtain the filtering density under the heavily-contaminated setting where optimal filters struggle to perform. We compare our scheme for a large range of β to the standard BPF with a Gaussian likelihood (BPF), as well as the (optimal) Kalman filter.

We shed light onto three questions on this simple setup: (a) Does the β -BPF produce an accurate and well-calibrated posterior distribution in the presence of contaminated data? (b) Is it sensitive to the choice β ? (c) Does the method described in Section 3.3 for selecting β return a near optimal result?

Figure 1 shows the results for $p_c = 0.1$. We observe that (a) the β -BPF outperforms the Kalman filter and the standard BPF for $\beta \leq 0.2$ while producing well-calibrated posteriors accounting for the uncertainty (for $\beta \in [0.01, 0.2]$ the coverage approaches the 90% threshold), (b) we see drastic performance gains (with median NMSE scores around $10\times$ smaller than the BPF and $100\times$ smaller than the Kalman filter) for a large range of β values, (c) we also see that the β -choice heuristic⁴ chooses a well-performing β (gold vertical lines in Figure 1).

⁴For simplicity, we apply it this choice criterion to the whole observation sequence seen by the filtering algorithm.

5.2 Terrain Aided Navigation

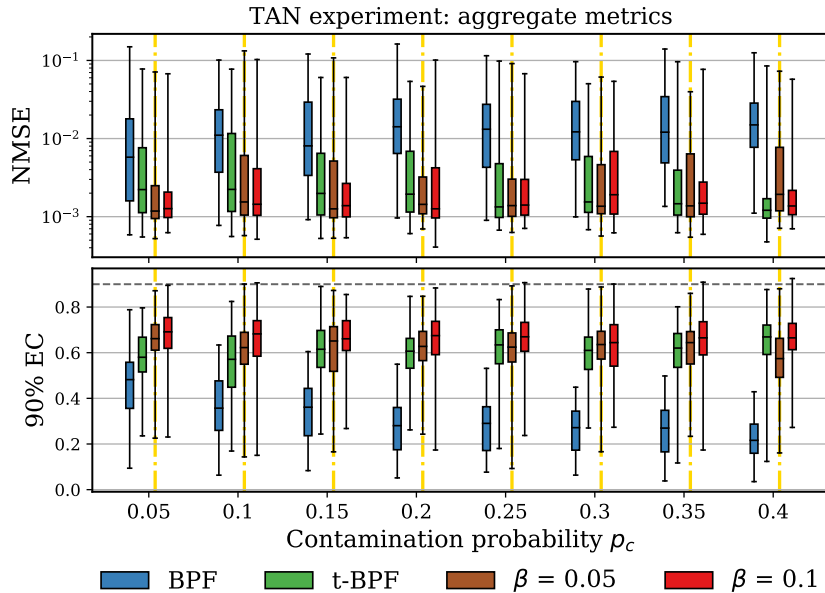


Figure 2: The mean metrics over state dimensions for the TAN example for different p_c . Only two values of β are shown to avoid visual clutter. The top panel presents the NMSE results (lower is better) and the bottom panel presents the 90% empirical coverage results (higher is better), both evaluated on 100 runs. The vertical dashed line in gold indicate the value of β chosen by the selection criterion in Section 3.3. The horizontal dashed line in black in the lower panel indicate the 90% mark for the coverage.

Terrain Aided Navigation (TAN) is a challenging estimation problem, where the state evolution is defined as in (25) (in three dimensions), but with a highly non-linear observation model,

$$\mathbf{y}_t = h(\mathbf{x}_t) + \boldsymbol{\epsilon}_t, \quad (27)$$

where $h(\cdot)$ is a non-linear function, typically including a non-analytic Digital Elevation Map (DEM). This problem simulates the trajectory of an airplane or a drone over a terrain map, where we observe its elevation over the terrain and its distance from its take-off hub from onboard sensors (see supplement for more details).

We simulate transmission failure of the measurement system as impulsive noise on the observations, i.e., i.i.d. draws from a Student's t distribution with $\nu = 1$ degrees of freedom. In other words, we define $\boldsymbol{\epsilon}_t \sim (1 - p_c)\mathcal{N}(0, 20^2) + p_c t_{\nu=1}(0, 20^2)$. We apply the β -BPF to this problem and compare it to the standard BPF with both Gaussian (BPF) and Student's t (t-BPF) likelihoods (as a standard alternative of using a heavy tailed likelihood, see, e.g., Xu et al. (2013)). We set the degrees of freedom for the t-BPF to the same value as the contamination $\nu = 1$.

From Figure 2, we observe that for low contamination, the β -BPF outperforms the standard Gaussian BPF and the t-BPF. This shows that the use of t -distribution for the low contamination setting is inappropriate. This gap in the performance tightens, naturally, as p_c grows since t -distribution becomes a good model for the observations.

However, in practice one might one to tune β on a sub-sequence to avoid extra computation.

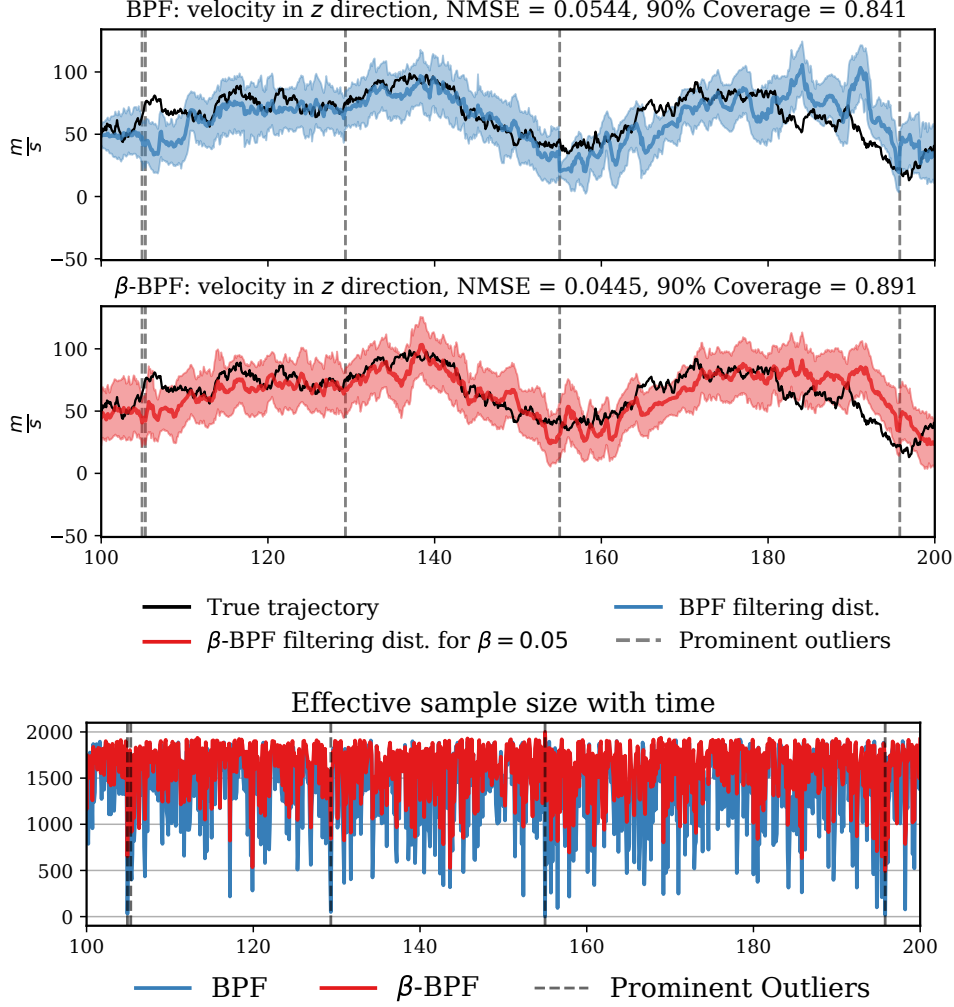


Figure 3: The top panel shows the inferred marginal filtering distributions for the velocity in the z direction for the BPF and β -BPF with $\beta = 0.05$. The lower panel shows the effective sample size with time. The locations of the most prominent (largest deviation) outliers are shown as dashed vertical lines in black in both panels.

In Figure 3, we plot the filtering distributions for the sixth state dimension (vertical velocity) obtained from an illustrative run with $p_c = 0.1$. The top panel shows the filtering distributions from the (Gaussian) BPF (up) and the β -BPF (down). The locations of the most prominent outliers are marked with dashed vertical lines in black. Figure 3 displays the significant difference between the two approaches: while the uncertainty for the standard BPF collapses when it meets the outliers, e.g. around $t = 155$, the β -BPF does not suffer from this problem. This performance difference is partly related to the stability of the weights. The lower panel in Figure 3 demonstrates the effective sample size (ESS) with time for the two filters showing precisely that the β -BPF consistently exhibits larger ESS values, avoiding particle degeneracy. The ESS values for the BPF, on the other hand, sharply decline when it meets outliers.

Asymmetric Wiener velocity: aggregate metrics for $p_c = 0.1$

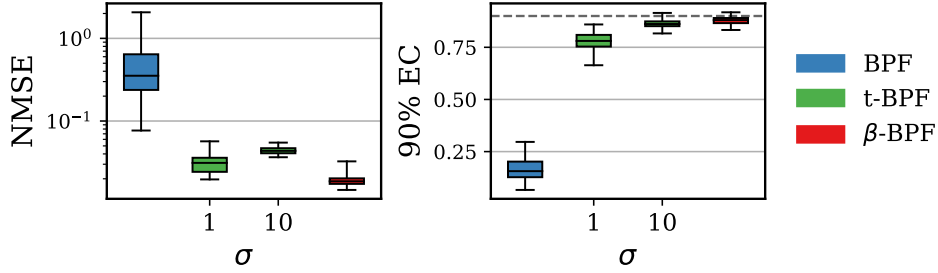


Figure 4: The mean metrics over state dimensions for the asymmetric Wiener velocity example with $p_c = 0.1$. The left panel presents the NMSE results (lower is better) and the right panel presents the 90% empirical coverage results (higher is better), both evaluated on 100 runs. The x -axis ticks indicate the scale used for Student’s t likelihood. The horizontal dashed line in black in the right panel indicates the 90% mark for the coverage.

5.3 Asymmetric Wiener velocity

In the case of simple, symmetric noise settings with additive contamination the use of heavy-tailed likelihoods such as Student’s t may be still seen as a viable alternative to robustify the inference. However, there are some realistic settings in which such off-the-shelf heavy-tailed replacements are not feasible or require considerable model-specific work. Consider, as a simple illustration, the Wiener velocity example in Section 5.1, where the observation noise in (26) is replaced with

$$\epsilon_t \sim \mathbb{1}_{[-\infty, 0]} \mathcal{N}(0, 1) + \mathbb{1}_{[0, +\infty]} \mathcal{N}(0, 10^2). \quad (28)$$

This simulates an asymmetric noise scenario. The observations are further contaminated with multiplicative exponential noise, i.e. $\epsilon_t \leftarrow \xi \epsilon_t$, for $\xi \sim \text{Exp}(1000)$ with probability p_c . This sums up to a multiplicatively corrupted asymmetric noise distribution which could, for example, represent a sensor with asymmetric noise profile in a failing regime which occasionally exhibits excessive gain.

For this example, it is easy to derive a BPF with the likelihood in (28). It is also easy to extend this likelihood to the β -BPF case. We test BPF and the β -BPF ($\beta = 0.1$) versus two versions of the t-BPF, in which the likelihood is replaced with a heavy-tailed symmetric one, one set to a short scale $\sigma = 1$ and the other set to a long scale $\sigma = 10$.

Figure 4 shows the results for this experiment. The BPF is unable to handle the multiplicative exponential contamination, as can be seen by the NMSE values. It also provides poor posterior coverage. The t-BPF fares better with this type of contamination where we can see a trade-off between accuracy and coverage depending on the chosen scale of the likelihood. This is due to the symmetry of the t -distribution which overestimates one of the tails depending on the scale. The β -BPF does not have this trade-off and outperforms the t-BPF on both metrics.

While one might attempt to model the noise with an asymmetric construction of the t -distributions which approximates the noise structure, we argue that in more general settings using heavy-tailed distributions requires approximations of the noise structure and making modelling choices which could be arbitrarily complex. This is in contrast to specifying a single tuning parameter as in the β -divergence case. The β -BPF requires no further modelling than the original problem and can be used as a drop-in replacement for nearly all types of likelihood structures.

5.4 London air quality Gaussian process regression

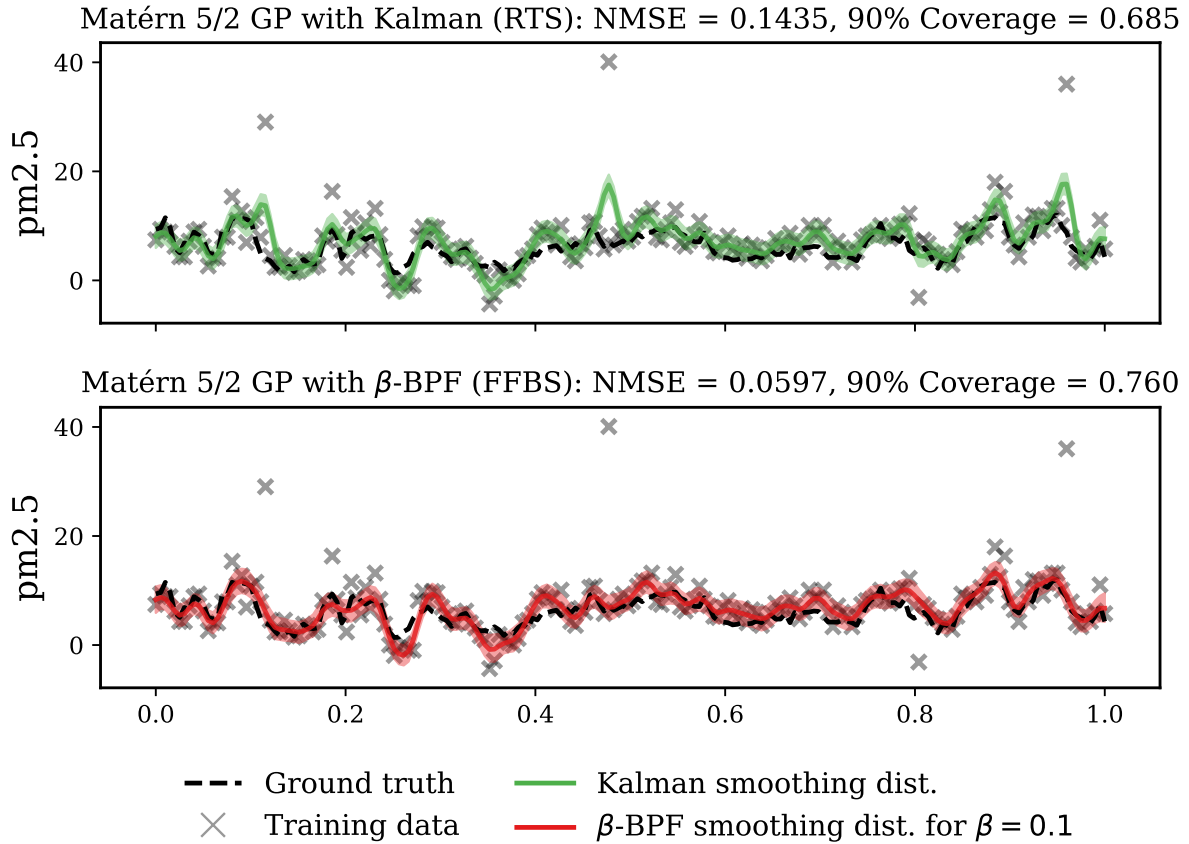


Figure 5: The GP fit on the measurement time series for one of the London air quality sensors. The top panel shows the posterior from the Kalman (RTS) smoothing. The bottom panel shows the posterior from the β -BPF (FFBS) for $\beta = 0.1$. The Kalman (RTS) solution is sensitive to the outliers forcing the GP mean towards them, while the β -BPF (FFBS) solution is robust.

To measure air quality, London authorities use a network of sensors around the city recording pollutant measurements. Sensor measurements are susceptible to significant outliers due to the dynamic nature of the environment around them, e.g. a truck passing by at the time of recording the measurement can generate a significant deviation from the usual observation characteristics. In the experiment, we use Gaussian process (GP) regression to infer the underlying signal from a PM2.5 sensor.

GPs are powerful smoothing and prediction tools, but they are notoriously computationally expensive ($\mathcal{O}(n^3)$) for closed form posterior inference. For one-dimensional time series data, one way to accelerate GP inference to linear time is to formulate an equivalent stochastic differential equation whose solution precisely matches the GP under consideration⁵ (Särkkä et al., 2013). The resulting model is a LGSSM of the form (25)–(26) where the smoothing distribution matches the GP marginals at discrete-times. One can then apply smoothing algorithms, such as the Rauch

⁵The SDE representation of a GP depends on the form of the covariance function. In this paper we use a GP with the Matérn 5/2 kernel, which admits a dual SDE representation.

Table 1: GP regression NMSE (higher is better) and 90% empirical coverage for the credible intervals of the posterior predictive distribution, on 100 runs. The **bold font** indicate the statistically significant best result according to the Wilcoxon signed-rank test. All presented results are statistically different from each other according to the test.

Filter (Smoother)	median (IQR)	
	NMSE	EC
Kalman (RTS)	0.144(0)	0.685(0)
BPF (FFBS)	0.116(0.015)	0.650(0.020)
($\beta = 0.1$)-BPF (FFBS)	0.061(0.003)	0.760(0.015)
($\beta = 0.2$)-BPF (FFBS)	0.059(0.002)	0.803(0.020)

Tung Striebel (RTS) (Rauch et al., 1965) or the Forward Filters Backward Smoothing (FFBS) (Briers et al., 2010) algorithms, to obtain the GP posterior. These algorithms require a forward filtering step with the Kalman filter for RTS or a PF for FFBS. Here, we fit a Matérn 5/2 GP with known hyperparameters to a time series from one of the sensors. For ground truth comparison, we aggregate the signals from the wider sensor network with the median to obtain a smooth signal.

Table 1 compares the results for the GP regression for the Kalman (RTS) smoothing, the standard BPF (FFBS) with Gaussian likelihood and two runs for the β -BPF (FFBS) with Gaussian likelihood for $\beta = 0.1$ – obtained from predictive selection as Section 3.3 – and $\beta = 0.2$ – overall best performing. We can see that for both choices of β , the β -BPF outperforms the other methods on both metrics.

To further investigate the GP solution of the β -BPF (FFBS), we show the fit for $\beta = 0.1$ and compare it with Kalman (RTS) smoothing. This is shown in Figure 5, where we can see that the Kalman (RTS) smoother is sensitive to outliers forcing the GP mean towards them. The β -BPF is robust in this case ignoring the influence from the outliers.

6 Conclusions

We provided a generalized filtering framework based on the idea of generalized Bayesian inference, which tackles likelihood misspecification in general state-space HMMs. Our approach leverages sequential Monte Carlo sampling methods, where we extended some analytical results to the generalized case. We presented the β -BPF, a simple instantiation of our approach based on the the β -divergence, and showed performance gains compared to other standard algorithms on a variety of problems and contamination settings.

References

- Ö. D. Akyildiz and J. Míguez. Nudging the particle filter. *Statistics and Computing*, 30:305–330, 2020.
- B. D. Anderson and J. B. Moore. *Optimal filtering*. Englewood Cliffs, N.J. Prentice Hall, 1979.
- A. Beskos, O. Papaspiliopoulos, G. O. Roberts, and P. Fearnhead. Exact and computationally efficient likelihood-based estimation for discretely observed diffusion processes. *Journal of the Royal Statistical Society, Series B*, 68(3):333–382, 2006.

- P. G. Bissiri, C. C. Holmes, and S. G. Walker. A general framework for updating belief distributions. *Journal of the Royal Statistical Society: Series B (Statistical Methodology)*, 78(5):1103–1130, 2016.
- M. Briers, A. Doucet, and S. Maskell. Smoothing algorithms for state space models. *Annals of the Institute of Statistical Mathematics*, 62(1):61–89, 2010.
- L. E. Calvet, V. Czellar, and E. Ronchetti. Robust filtering. *Journal of the American Statistical Association*, 110(512):1591–1606, Dec. 2015.
- N. Chopin. Central limit theorem for sequential Monte Carlo methods and its application to Bayesian inference. *The Annals of Statistics*, 32(6):2385–2411, 2004.
- A. Cichocki and S.-i. Amari. Families of alpha-beta-and gamma-divergences: Flexible and robust measures of similarities. *Entropy*, 12(6):1532–1568, 2010.
- P. Del Moral. *Feynman-Kac formulae: Genealogical and interacting particle systems with applications*. Springer, 2004.
- A. Doucet and A. M. Johansen. A tutorial on particle filtering and smoothing: Fifteen years later. In D. Crisan and B. Rozovskiĭ, editors, *The Oxford Handbook of Nonlinear Filtering*, pages 656–704. Oxford University Press, 2011.
- A. Doucet, S. Godsill, and C. Andrieu. On sequential Monte Carlo sampling methods for Bayesian filtering. *Statistics and Computing*, 10(3):197–208, 2000.
- P. Fearnhead, O. Papaspiliopoulos, and G. O. Roberts. Particle filters for partially-observed diffusion. *Journal of the Royal Statistical Society, Series B*, 70(4):755–777, 2008.
- F. Futami, I. Sato, and M. Sugiyama. Variational inference based on robust divergences. In *International Conference on Artificial Intelligence and Statistics*, pages 813–822, 2018.
- M. Gerber, N. Chopin, and N. Whiteley. Negative association, ordering and convergence of resampling methods. *Annals of Statistics*, 47(4):2236–2260, 2019.
- A. Ghosh and A. Basu. Robust Bayes estimation using the density power divergence. *Annals of the Institute of Statistical Mathematics*, 68(2):413–437, 2016.
- N. J. Gordon, D. J. Salmond, and A. F. Smith. Novel approach to nonlinear/non-Gaussian Bayesian state estimation. *IEE proceedings F (radar and signal processing)*, 140(2):107–113, 1993.
- X.-L. Hu, T. B. Schon, and L. Ljung. A robust particle filter for state estimation—with convergence results. In *2007 46th IEEE Conference on Decision and Control*, pages 312–317. IEEE, 2007.
- P. J. Huber. *Robust statistics*. Springer, 2011.
- J. Jewson, J. Smith, and C. Holmes. Principles of Bayesian inference using general divergence criteria. *Entropy*, 20(6):442, 2018.
- A. M. Johansen and A. Doucet. A note on the auxiliary particle filter. *Statistics and Probability Letters*, 78(12):1498–1504, September 2008.
- R. E. Kalman. A new approach to linear filtering and prediction problems. *Journal of Fluids Engineering*, 82(1):35–45, 1960.

- J. Knoblauch, J. E. Jewson, and T. Damoulas. Doubly robust Bayesian inference for non-stationary streaming data with β -divergences. In *Advances in Neural Information Processing Systems*, pages 64–75, 2018.
- J. Knoblauch, J. Jewson, and T. Damoulas. Generalized Variational Inference: Three arguments for deriving new Posteriors. *arXiv preprint arXiv:1904.02063*, 2019.
- C. S. Maiz, J. Miguez, and P. M. Djuric. Particle filtering in the presence of outliers. In *2009 IEEE/SP 15th Workshop on Statistical Signal Processing*, pages 33–36. IEEE, 2009.
- C. S. Maiz, E. M. Molanes-Lopez, J. Miguez, and P. M. Djuric. A particle filtering scheme for processing time series corrupted by outliers. *IEEE Transactions on Signal Processing*, 60(9): 4611–4627, 2012.
- J. Míguez, D. Crisan, and P. M. Djurić. On the convergence of two sequential Monte Carlo methods for maximum a posteriori sequence estimation and stochastic global optimization. *Statistics and Computing*, 23(1):91–107, 2013.
- H. E. Rauch, F. Tung, and C. T. Striebel. Maximum likelihood estimates of linear dynamic systems. *AIAA journal*, 3(8):1445–1450, 1965.
- S. Särkkä. *Bayesian Filtering and Smoothing*. Cambridge University Press, 2013.
- S. Särkkä and A. Solin. *Applied Stochastic Differential Equations*, volume 10. Cambridge University Press, 2019.
- S. Särkkä, A. Solin, and J. Hartikainen. Spatiotemporal learning via infinite-dimensional Bayesian filtering and smoothing: A look at Gaussian process regression through Kalman filtering. *IEEE Signal Processing Magazine*, 30(4):51–61, 2013.
- F. C. Teixeira, J. Quintas, P. Maurya, and A. Pascoal. Robust particle filter formulations with application to terrain-aided navigation. *International Journal of Adaptive Control and Signal Processing*, 31(4):608–651, 2017.
- J. von Neumann and O. Morgenstern. *Theory of Games and Economic Behavior*. Princeton University Press, 1947.
- D. Xu, C. Shen, and F. Shen. A robust particle filtering algorithm with non-Gaussian measurement noise using student-t distribution. *IEEE Signal Processing Letters*, 21(1):30–34, 2013.
- A. Zellner. Optimal information processing and Bayes’s theorem. *The American Statistician*, 42(4):278–280, 1988.

Supplementary Material

A β -BPF

A.1 Outline derivation of the loss in (19)

To arrive at the expression of the loss in (19), recall the formula for the beta divergence (Cichocki and Amari, 2010)

$$\begin{aligned} D_B^\beta(\mathbf{P}||\mathbf{Q}) &= \frac{1}{\beta(\beta+1)} \int (p^{\beta+1}(x) + \beta q^{\beta+1}(x) - (\beta+1)p(x)q^\beta(x)) d\mu(x) \\ &= C_{\mathbf{P}} + \frac{1}{\beta+1} \int q^{\beta+1}(x) dx - \frac{1}{\beta} \int q(x) \mathbf{P}(dx) \end{aligned}$$

where \mathbf{P} and \mathbf{Q} are probability measures on the measurable space (X, \mathcal{A}) and μ is a finite or σ -finite measure on this space, such that $\mathbf{P} \ll \mu$ and $\mathbf{Q} \ll \mu$ are absolutely continuous w.r.t. μ and $C_{\mathbf{P}}$ is a constant independent of \mathbf{Q} . Finally, $p = \frac{d\mathbf{P}}{d\mu}$ and $q = \frac{d\mathbf{Q}}{d\mu}$ are densities and the Radon-Nikodym derivatives for \mathbf{P} and \mathbf{Q} w.r.t. μ .

Comparison with (7) yields (11) directly.

A.2 Algorithm

Here, we provide the algorithmic procedure in Algorithm 2 for the β -BPF that is used investigated in this main text.

Algorithm 2 β -Bootstrap Particle Filter

Input: Observation sequence $\mathbf{y}_{1:T}$, number of samples N .

Initialise: Sample $\{\bar{\mathbf{x}}_0^{(i)}\}_{i=1}^N$ for the prior $\pi_0(\mathbf{x}_0)$.

for $t = 1$ **to** T **do**

Sample:

$$\tilde{\mathbf{x}}_t^{(i)} \sim f_t(\mathbf{x}_t | \bar{\mathbf{x}}_{t-1}^{(i)}) \quad \text{for } i = 1, \dots, N.$$

Weight:

$$w_t^{(i)} \propto G_t^\beta(\tilde{\mathbf{x}}_t^{(i)}) \quad \text{for } i = 1, \dots, N.$$

Resample:

$$\bar{\mathbf{x}}_t^{(i)} \sim \sum_{i=1}^N w_t^{(i)} \delta_{\tilde{\mathbf{x}}_t^{(i)}}(d\mathbf{x}_t) \quad \text{for } i = 1, \dots, N.$$

end for

B Theoretical analysis

B.1 Proof of Theorem 1

This is an adaptation of a well-known proof, hence we will sketch results and provide the constant $c_{t,p,\beta}$.

The result is proved via induction. For $t = 0$, we have the result in the theorem trivially, as it corresponds to the i.i.d. case and, e.g. [Del Moral \(2004, Lemma 7.3.3\)](#) provides an explicit constant. Hence, as an induction hypothesis, we assume

$$\|\pi_{t-1}^{\beta,N}(\varphi) - \pi_{t-1}^{\beta}(\varphi)\|_p \leq \frac{c_{t-1,p,\beta} \|\varphi\|_{\infty}}{\sqrt{N}}, \quad (29)$$

where $c_{t-1,p,\beta} < \infty$ is independent of N . After the sampling step, we obtain the predictive particles $\bar{\mathbf{x}}_t^{(i)}$ and form the predictive measure

$$\bar{\pi}_t^{\beta,N}(\mathrm{d}\mathbf{x}_t | y_{1:t-1}) = \frac{1}{N} \sum_{i=1}^N \delta_{\bar{\mathbf{x}}_t^{(i)}}(\mathrm{d}\mathbf{x}_t),$$

and then one can show that we have ([Míguez et al., 2013, Lemma 1](#))

$$\|\bar{\pi}_t^{\beta,N}(\varphi) - \bar{\pi}_t^{\beta}(\varphi)\|_p \leq \frac{c_{1,t,p,\beta} \|\varphi\|_{\infty}}{\sqrt{N}}, \quad (30)$$

where $c_{1,t,p,\beta} < \infty$ is a constant independent of N . After the computation of weights, we construct

$$\tilde{\pi}_t^{\beta,N}(\mathrm{d}\mathbf{x}_t) = \sum_{i=1}^N w_t^{(i)} \delta_{\bar{\mathbf{x}}_t^{(i)}}(\mathrm{d}\mathbf{x}_t). \quad (31)$$

Following again ([Míguez et al., 2013, Lemma 1](#)), one readily obtains

$$\|\pi_t^{\beta}(\varphi) - \tilde{\pi}_t^{\beta,N}(\varphi)\|_p \leq \frac{c_{2,t,p,\beta} \|\varphi\|_{\infty}}{\sqrt{N}}, \quad (32)$$

where

$$c_{2,t,p,\beta} = \frac{2 \|G_t^{\beta}\|_{\infty} c_{1,t,p,\beta}}{\bar{\pi}_t(G_t^{\beta})} < \infty,$$

where we note $\bar{\pi}_t(G_t^{\beta}) > 0$. Finally, performing multinomial resampling leads to a conditionally-i.i.d. sampling case, which yields

$$\|\tilde{\pi}_t^{\beta,N}(\varphi) - \pi_t^{\beta,N}(\varphi)\|_p \leq \frac{c_{3,t,p,\beta} \|\varphi\|_{\infty}}{\sqrt{N}}. \quad (33)$$

Combining (32) and (33) yields the result with $c_{t,p,\beta} = c_{2,t,p,\beta} + c_{3,t,p,\beta}$.

B.2 Proof of Theorem 2

We refer to the Proposition in [Johansen and Doucet \(2008\)](#) which provides explicit expressions for sequential importance resampling based particle filters within the general frameworks of [Del Moral \(2004\)](#), [Chopin \(2004\)](#); the same argument holds *mutatis mutandis* in the context of

the β -BPF. We note that the asymptotic variance expression $\sigma_{t,\beta}^2(\varphi)$ is given as follows. For $t = 1$, we obtain (Johansen and Doucet, 2008)

$$\sigma_{1,\beta}^2(\varphi) = \int \frac{p_1^\beta(\mathbf{x}_1|\mathbf{y}_1)}{f_1(\mathbf{x}_1)} (\varphi_1(\mathbf{x}_1) - \bar{\varphi}_1)^2 d\mathbf{x}_1,$$

where $f_1(\mathbf{x}_1) := \int \mu_0(\mathbf{x}_0) f_1(\mathbf{x}_1|\mathbf{x}_0) d\mathbf{x}_0$. Then, for $t > 1$ (Johansen and Doucet, 2008)

$$\begin{aligned} \sigma_{t,\beta}^2 &= \int \frac{p_t^\beta(\mathbf{x}_1|\mathbf{y}_{1:t})^2}{f_1(\mathbf{x}_1)} \left(\int \varphi_t(\mathbf{x}_{1:t}) p_t^\beta(\mathbf{x}_{2:t}|\mathbf{y}_{2:t}, \mathbf{x}_1) d\mathbf{x}_{2:t} - \bar{\varphi}_t \right)^2 d\mathbf{x}_1 \\ &+ \sum_{k=2}^{t-1} \int \frac{p_k^\beta(\mathbf{x}_{1:k}|\mathbf{y}_{1:t})^2}{p_{k-1}^\beta(\mathbf{x}_{1:k-1}|\mathbf{y}_{1:k-1}) f_k(\mathbf{x}_k|\mathbf{x}_{k-1})} \left(\int \varphi_t(\mathbf{x}_{1:t}) p_t^\beta(\mathbf{x}_{k+1:t}|\mathbf{y}_{k+1:t}, \mathbf{x}_k) d\mathbf{x}_{k+1:t} - \bar{\varphi}_t \right)^2 d\mathbf{x}_{1:k} \\ &+ \int \frac{p_t^\beta(\mathbf{x}_{1:t}|\mathbf{y}_{1:t})^2}{p_{t-1}^\beta(\mathbf{x}_{1:t-1}|\mathbf{y}_{1:t-1}) f_t(\mathbf{x}_t|\mathbf{x}_{t-1})} (\varphi_t(\mathbf{x}_{1:t}) - \bar{\varphi}_t)^2 d\mathbf{x}_{1:t}. \end{aligned}$$

C Experiment Details

C.1 Evaluation Metrics

The following metrics are used to evaluate the experiments:

The Normalised Mean Squared Error (NMSE) is computed per state dimension j as

$$\text{NMSE}_j = \frac{\left\| \sum_{t=1}^T x_{tj} - \hat{x}_{tj} \right\|_2^2}{\sum_{t=1}^T \|x_{tj}\|_2^2}, \quad (34)$$

with $\hat{x}_{tj} = \frac{1}{N} \sum_{i=1}^N \bar{x}_{tj}^{(i)}$, i.e. the mean over resampled particles (trajectories).

The 90% Empirical Coverage (EC) is computed per state dimension j as

$$\text{EC}_j = \frac{\sum_{t=1}^T \mathbb{1}_{C_t}(x_{tj})}{T}, \quad (35)$$

with

$$C_t = \{z | z \in [\mathfrak{q}_{0.05}(\{\bar{x}_{tj}^{(i)}\}_{i=1}^N), \mathfrak{q}_{0.95}(\{\bar{x}_{tj}^{(i)}\}_{i=1}^N)]\},$$

where \mathfrak{q} is the quantile function.

Aggregation: Metrics are often presented as aggregates over the state dimensions, which are simply the mean of the metric across the state dimensions.

C.2 Details on the implementation of the selection criterion in Section 3.3

From (21), we chose agg as the median and \mathcal{L} as the absolute error. When the observations are multidimensional, we take the average loss weighted by the inverse of the median of each dimension.

We compute the score for different values of β from a grid and choose β that minimises the score. For multiple runs, we report the modal value of the β 's over all the runs.

In the interest of simplicity, we use the entire observation sequence to compute the score. However, in practice one might tune β on a sub-sequence to avoid extra computation.

C.3 Wiener velocity model experiment details (Section 5.1)

In this section, we detail the experimental setup used to obtain the results for Section 5.1.

Simulator settings We synthesise the data with a Python simulator utilising NumPy. We discretise the system with $\Delta\tau = 0.1$ and simulate it for 100 time steps, i.e. we obtain 1000 time points in total. For the state evolution process in Equation (25), we set the transition

matrix $\mathbf{A} = \begin{bmatrix} 1 & 0 & \Delta\tau & 0 \\ 0 & 1 & 0 & \Delta\tau \\ 0 & 0 & 1 & 0 \\ 0 & 0 & 0 & 1 \end{bmatrix}$ and the transition covariance matrix $\mathbf{Q} = \begin{bmatrix} \frac{\Delta\tau^3}{3} & 0 & \frac{\Delta\tau^2}{2} & 0 \\ 0 & \frac{\Delta\tau^3}{3} & 0 & \frac{\Delta\tau^2}{2} \\ \frac{\Delta\tau^2}{2} & 0 & \Delta\tau & 0 \\ 0 & \frac{\Delta\tau^2}{2} & 0 & \Delta\tau \end{bmatrix}$. For the

observation process in Equation (26), we set the observation matrix $\mathbf{H} = \begin{bmatrix} 1 & 0 & 0 & 0 \\ 0 & 1 & 0 & 0 \end{bmatrix}$ and the noise covariance $\Sigma = \mathbf{I}$. The initial state of the simulator is set to $\mathbf{x}_0 = [140, 140, 50, 0]$.

Contamination To simulate contaminated observations we apply extra i.i.d. Gaussian noise with a standard deviation of 100.0 to the observation sequence with probability p_c per observation.

Sampler settings We initialise the samplers by sampling from the prior given by $\mathcal{N}(\mathbf{x}_0, \mathbf{Q})$ with \mathbf{x}_0 being the initial state of the simulator and \mathbf{Q} as above. We set the likelihood covariance to the simulator noise covariance and the number of samples to 1000.

Experiment settings Each experiment consists of 100 runs, where all samplers are seeded with the same seed per run; however, the seeds vary across the runs. We use the same state sequence for all runs obtained from the simulator as above. However, each run simulates a new observation sequence (i.e. the observations noise changes per run).

C.4 Terrain Aided Navigation (TAN) experiment details (Section 5.2)

In this section, we detail the experimental setup used to obtain the results for Section 5.2.

Simulator settings We synthesise the data with a Python simulator utilising NumPy. We discretise the system with $\Delta\tau = 0.1$ and simulate it for 200 time steps, i.e. we obtain 2000 time points in total. For the state evolution process in Equation (25), we set the transition matrix

$$\mathbf{A} = \begin{bmatrix} 1 & 0 & 0 & \Delta\tau & 0 & 0 \\ 0 & 1 & 0 & 0 & \Delta\tau & 0 \\ 0 & 0 & 1 & 0 & 0 & \Delta\tau \\ 0 & 0 & 0 & 1 & 0 & 0 \\ 0 & 0 & 0 & 0 & 1 & 0 \\ 0 & 0 & 0 & 0 & 0 & 1 \end{bmatrix},$$

and the transition covariance matrix

$$\mathbf{Q} = \begin{bmatrix} 4 & 0 & 0 & 0 & 0 & 0 \\ 0 & 4 & 0 & 0 & 0 & 0 \\ 0 & 0 & 36 & 0 & 0 & 0 \\ 0 & 0 & 0 & 0.0841 & 0 & 0 \\ 0 & 0 & 0 & 0 & 0.207936 & 0 \\ 0 & 0 & 0 & 0 & 0 & 5.29 \end{bmatrix}.$$

For the observation process in (27), we set the non-linear observation function

$$h(\mathbf{x}_t) = \left[\frac{x_{t3} - \text{DEM}(x_{t1}, x_{t2})}{\sqrt{(x_{t1} - x_{01})^2 + (x_{t2} - x_{02})^2}} \right],$$

where DEM is a non-analytic Digital Elevation Map. For our simulation we set DEM to

$$\text{DEM}(a, b) = \text{peaks}(q \cdot a, q \cdot b) + \sum_{i=1}^6 \alpha_i \sin(\omega_i \cdot q \cdot a) \cos(\psi \cdot q \cdot b),$$

with $\text{peaks}(c, d) = 200(3(1-c)^2 \exp(-c^2 - (d+1)^2) - 10(\frac{c}{5} - c^3 - d^5) \exp(-c^2 - d^2) - \frac{1}{3} \exp(-(x+1)^2 + y^2))$, $\boldsymbol{\alpha} = [300, 80, 60, 40, 20, 10]$, $\boldsymbol{\omega} = [5, 10, 20, 30, 80, 150]$, $\boldsymbol{\psi} = [4, 10, 20, 40, 90, 150]$ and $q = \frac{3}{2.96 \times 10^4}$. The noise covariance $\Sigma = \sigma^2 \mathbf{I}$ with $\sigma^2 = 400$. The initial state of the simulator is set $\mathbf{x}_0 = [-7.5 \times 10^3, 5 \times 10^3, 1.1 \times 10^3, 88.15, -60.53, 0]$.

Contamination To simulate contaminated observations we apply extra i.i.d. Student's t noise with 1 degree of freedom scale σ , where σ is given as above. The contamination is applied to observation instances with probability p_c per observation.

Sampler settings We initialise the samplers by sampling from the prior given by $\mathcal{N}(\mathbf{x}_0, \mathbf{Q})$ with \mathbf{x}_0 being the initial state of the simulator and \mathbf{Q} as above. We set the likelihood covariance to the simulator noise covariance and the number of samples to 1000.

Experiment settings Each experiment consists of 100 runs, where all samplers are seeded with the same seed per run; however, the seeds vary across the runs. We use the same state sequence for all runs obtained from the simulator as above. However, each run simulates a new observation sequence (i.e. the observation noise changes per run).

C.5 Asymmetric Wiener velocity model experiment details (Section 5.3)

In this section, we detail the experimental setup used to obtain the results for Section 5.3.

Simulator settings We use the same simulator settings as in Appendix C.3, but changing the observation noise to Equation (28).

Contamination To simulate contaminated observations we multiplicative apply i.i.d. Exponential noise with a scale of 1000 with probability $p_c = 0.1$ per observation.

Sampler settings We initialise the samplers by sampling from the prior given by $\mathcal{N}(\mathbf{x}_0, \mathbf{Q})$ with \mathbf{x}_0 being the initial state of the simulator and \mathbf{Q} as above. We set the number of samples to 1000.

Experiment settings We use the same settings as in Appendix C.3.

C.6 Air quality experiment details (Section 5.4)

In this section, we detail the setup used to obtain the results for Section 5.4.

Data The data was obtained from <https://www.londonair.org.uk/london/asp/datadownload.asp>. We select a time window of 200 hours. No preprocessing was performed on the data.

Kernel We use the Matérn 5/2 kernel and set the lengthscale $l = 0.03$ and the signal variance $\sigma_s^2 = 32$. We discretize the SDE representation of the Matérn 5/2 GP with stepsize $\Delta\tau = 0.005$ to obtain an LGSSM of the form (25)-(26), with transition matrix

$$\mathbf{A} = \exp(\Delta\tau\mathbf{F}) = \exp\left(\Delta\tau \begin{bmatrix} 0 & 1 & 0 \\ 0 & 0 & 1 \\ -\lambda^3 & -3\lambda^2 & -3\lambda \end{bmatrix}\right),$$

where $\lambda = \frac{\sqrt{5}}{l}$ and transition covariance matrix $\mathbf{Q} = \mathbf{P}_\infty - \mathbf{A}\mathbf{P}_\infty\mathbf{A}^\top$, with $\mathbf{P}_\infty = \begin{bmatrix} \sigma_s^2 & 0 & \kappa \\ 0 & \kappa & 0 \\ -\kappa & 0 & \sigma_s^2\lambda^4 \end{bmatrix}$,

where $\kappa = \frac{\sigma_s^2\lambda^2}{3}$. For the observation process in (26), the observation matrix is set to $\mathbf{H} = [1, 0, 0]$ and the noise variance $\sigma^2 = 1$. The prior on the initial state \mathbf{x}_x is given as $\mathcal{N}(m, S)$, where $m^\top = [0, 0, 0]$ and $S = \mathbf{P}_\infty$.

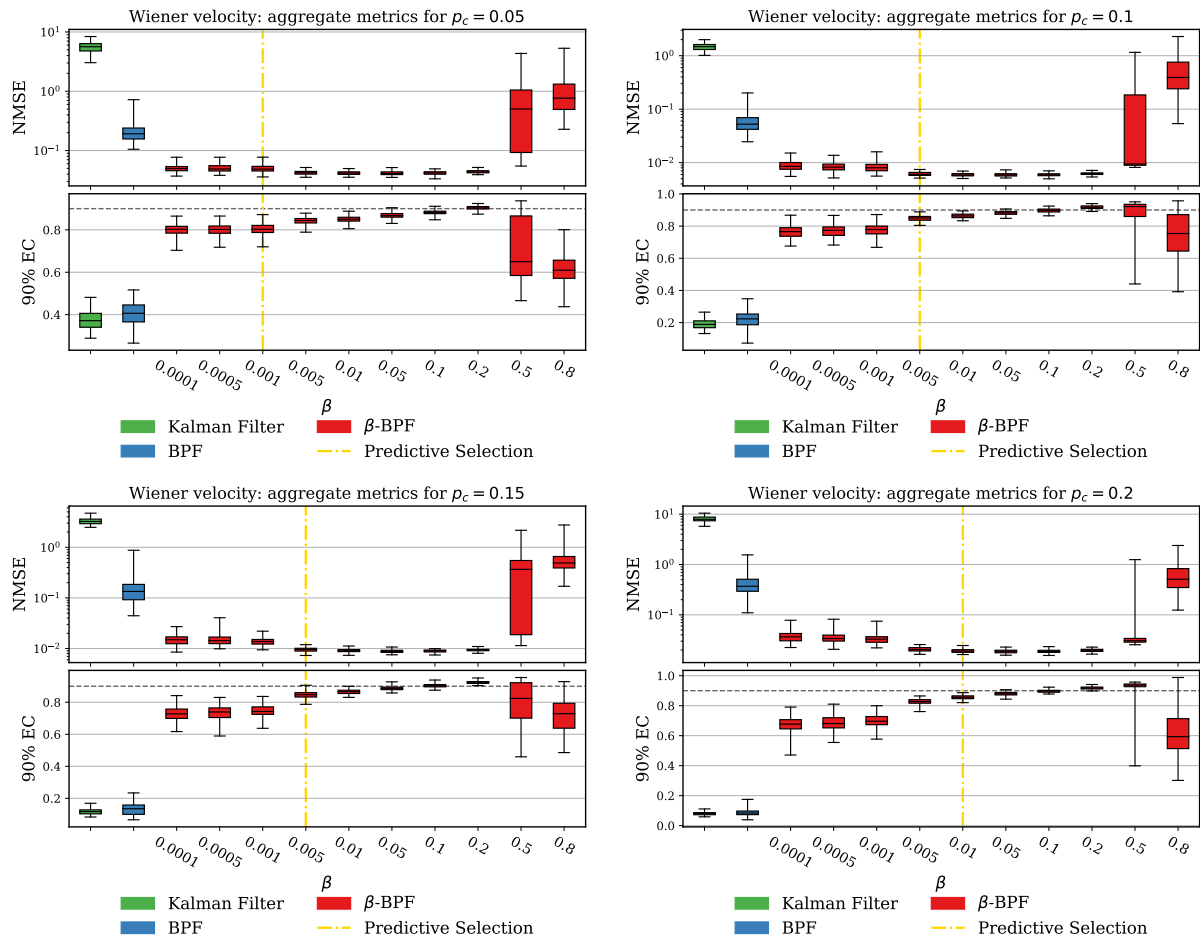
Sampler settings We initialise the samples by sampling from the prior $\mathcal{N}(m, S)$. We set the number of samples to 1000.

Smoother settings We set the number of samples to 1000 for the FFBS smoother.

Experiment settings We repeat the sampling procedure for 100 runs, where the samplers are seeded differently for each runs. The seeds are shared among samplers for each run. The Kalman filter does not require multiple runs as the solution is deterministic.

D Further results

D.1 Wiener velocity experiment



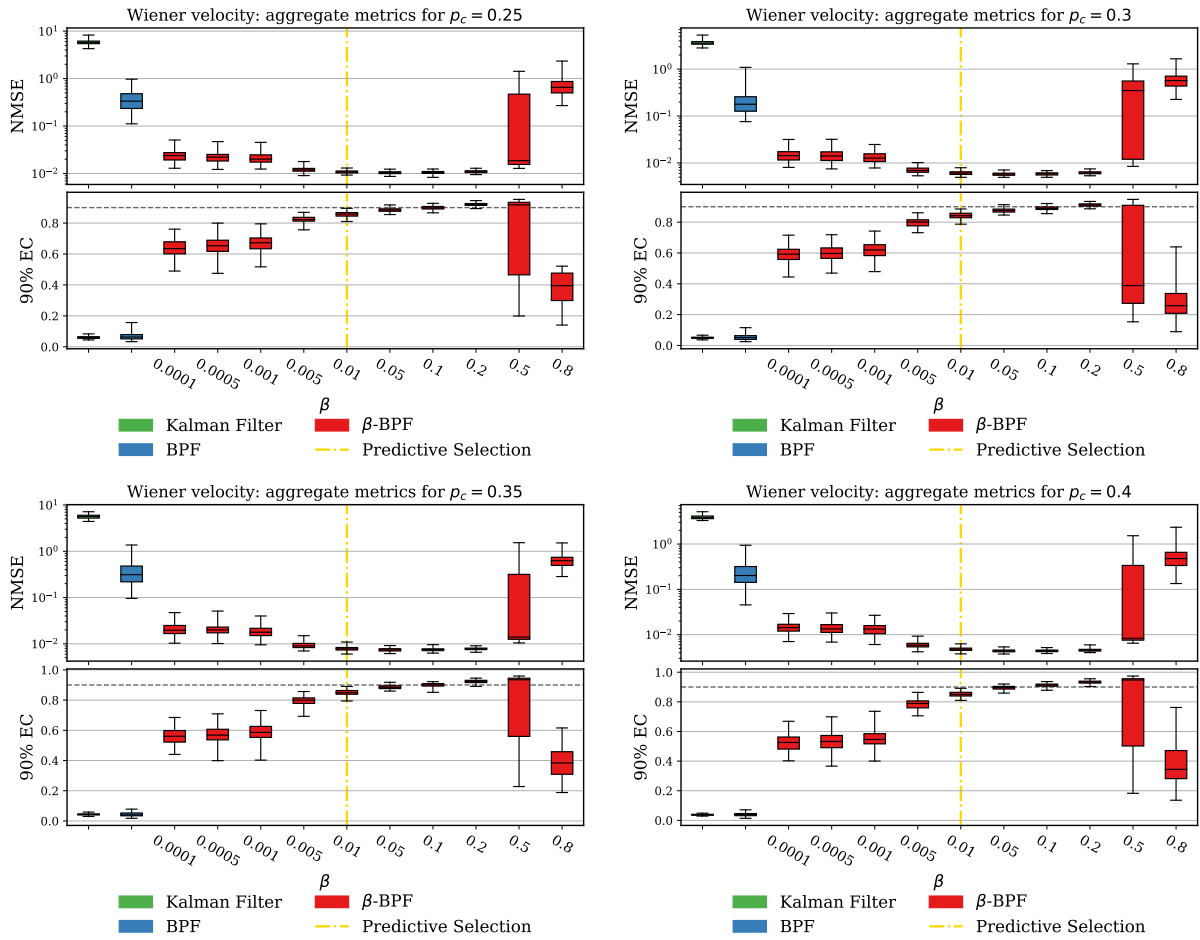


Figure 6: The mean metrics over state dimensions for the Wiener velocity example. The top panel presents the NMSE results (lower is better) and the bottom panel presents the 90% empirical coverage results (higher is better), on 100 runs. The vertical dashed line in gold indicate the value of β chosen by the selection criterion in Section 3.3. The horizontal dashed line in black in the lower panel indicates the 90% mark for the coverage.

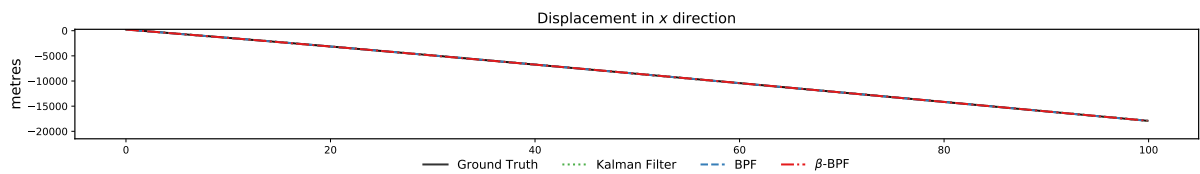


Figure 7: Marginal filtering distributions for the Kalman filter, the BPF and the β -BPF.

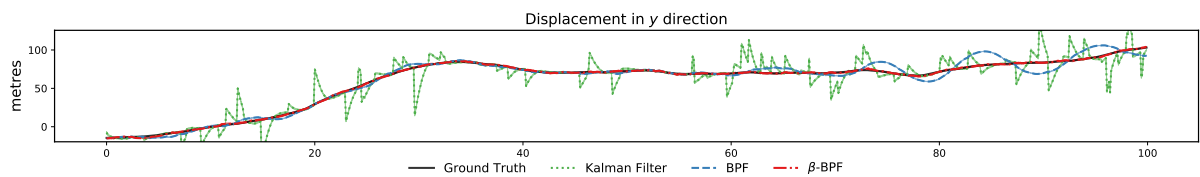


Figure 8: Marginal filtering distributions for the Kalman filter, the BPF and the β -BPF.

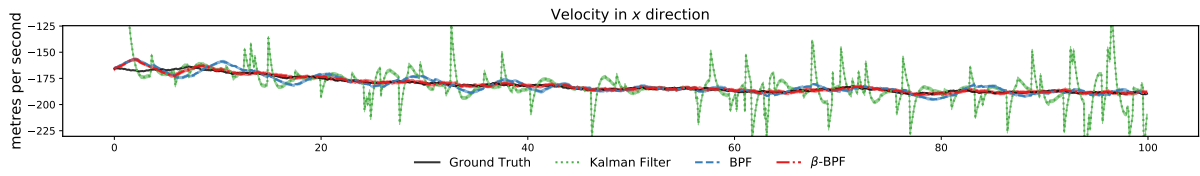


Figure 9: Marginal filtering distributions for the Kalman filter, the BPF and the β -BPF.

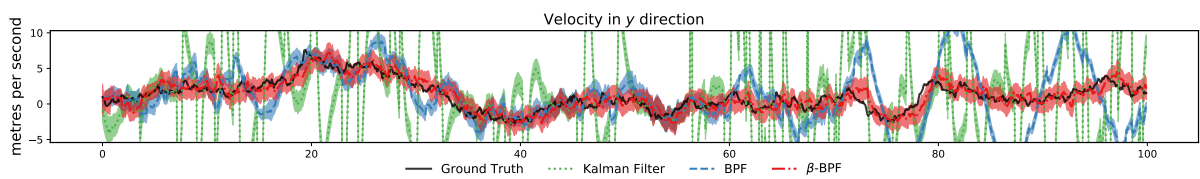


Figure 10: Marginal filtering distributions for the Kalman filter, the BPF and the β -BPF.

D.2 TAN experiment

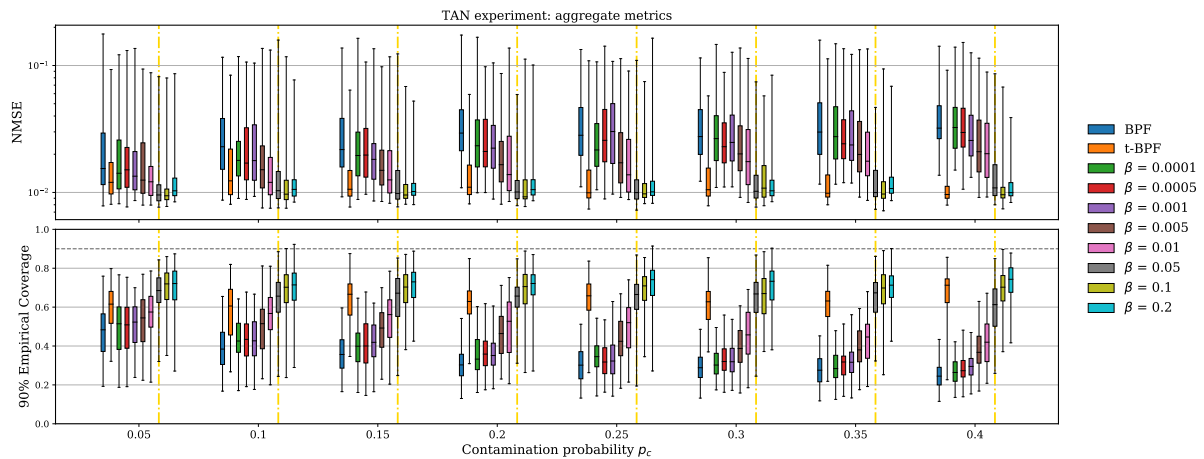


Figure 11: Expanded version of Figure 2 in the main text. Colour palette changed to accommodate the number of comparisons. See original caption for explanation of the figure.

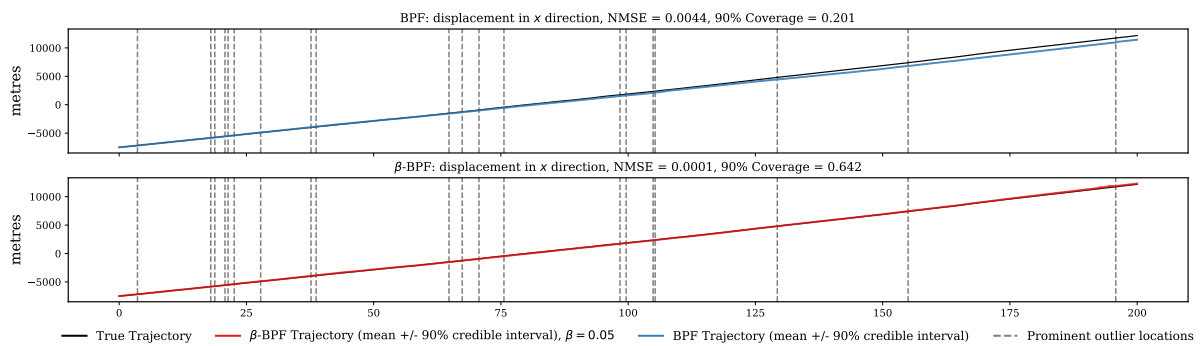


Figure 12: Marginal filtering distributions for the BPF (top) and β -BPF (bottom) with $\beta = 0.05$. The locations of the most prominent (largest deviation) outliers are shown as dashed vertical lines in black.

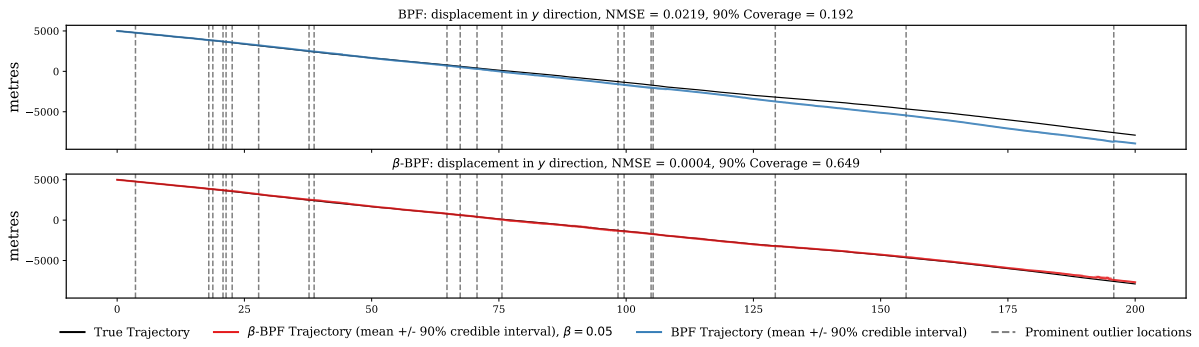


Figure 13: Marginal filtering distributions for the BPF (top) and β -BPF (bottom) with $\beta = 0.05$. The locations of the most prominent (largest deviation) outliers are shown as dashed vertical lines in black.

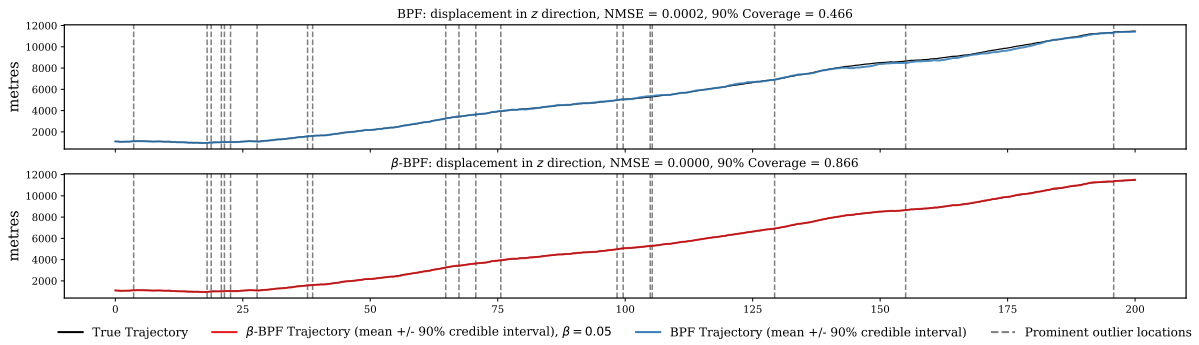


Figure 14: Marginal filtering distributions for the BPF (top) and β -BPF (bottom) with $\beta = 0.05$. The locations of the most prominent (largest deviation) outliers are shown as dashed vertical lines in black.

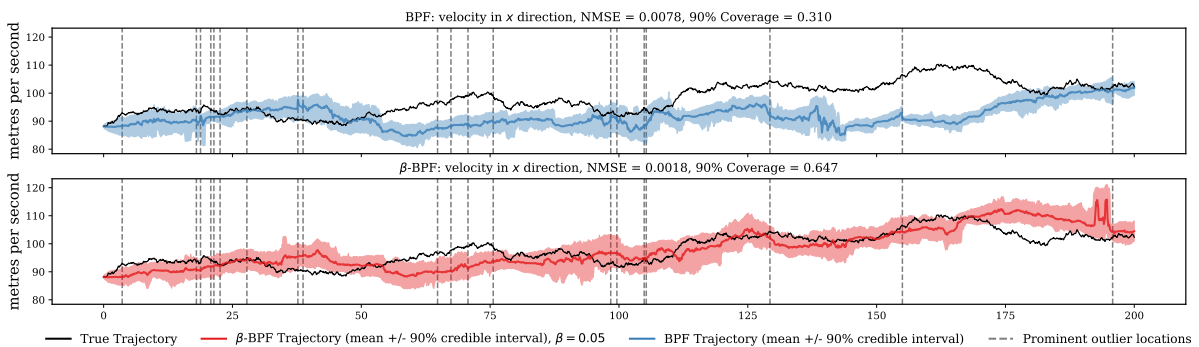


Figure 15: Marginal filtering distributions for the BPF (top) and β -BPF (bottom) with $\beta = 0.05$. The locations of the most prominent (largest deviation) outliers are shown as dashed vertical lines in black.

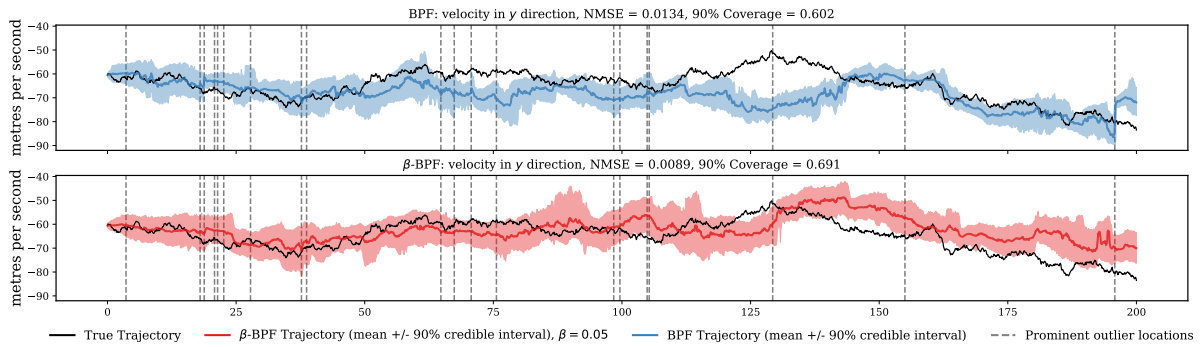


Figure 16: Marginal filtering distributions for the BPF (top) and β -BPF (bottom) with $\beta = 0.05$. The locations of the most prominent (largest deviation) outliers are shown as dashed vertical lines in black.

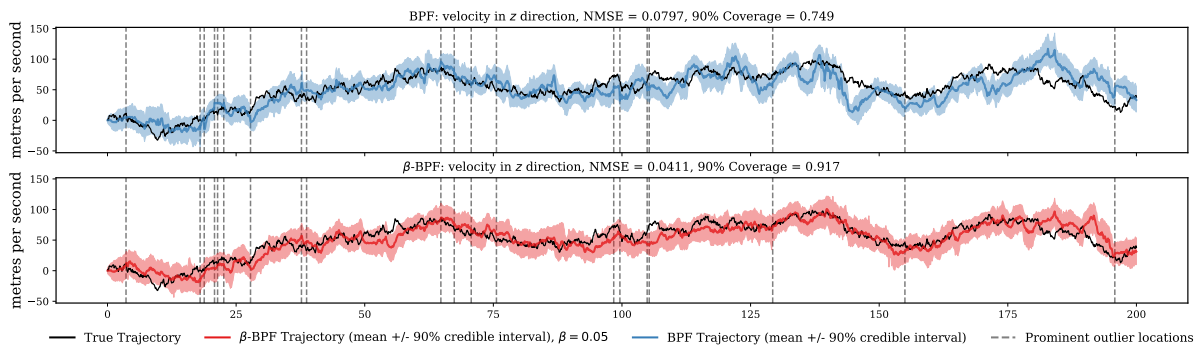


Figure 17: Marginal filtering distributions for the BPF (top) and β -BPF (bottom) with $\beta = 0.05$. The locations of the most prominent (largest deviation) outliers are shown as dashed vertical lines in black.

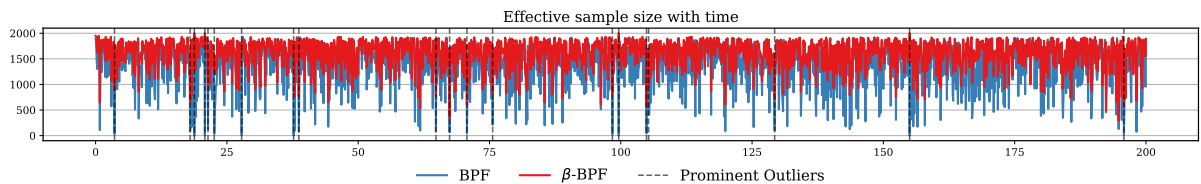


Figure 18: Effective sample size with time for the BPF (top) and β -BPF with $\beta = 0.05$.

D.3 London air quality experiment

Table 2: GP regression NMSE (higher is better) and 90% empirical coverage for the credible intervals of the posterior predictive distribution, on 100 runs. The **bold font** indicate the statistically significant best result according to the Wilcoxon signed-rank test. All presented results are statistically different from each other according to the test.

Filter (Smoother)	median (IQR)	
	NMSE	EC
Kalman (RTS)	0.144(0)	0.685(0)
BPF (FFBS)	0.116(0.015)	0.650(0.020)
($\beta = 0.005$)-BPF (FFBS)	0.102(0.014)	0.67(0.025)
($\beta = 0.01$)-BPF (FFBS)	0.077(0.007)	0.705(0.015)
($\beta = 0.05$)-BPF (FFBS)	0.063(0.003)	0.735(0.015)
($\beta = 0.1$)-BPF (FFBS)	0.061(0.003)	0.760(0.015)
($\beta = 0.2$)-BPF (FFBS)	0.059(0.002)	0.803(0.020)

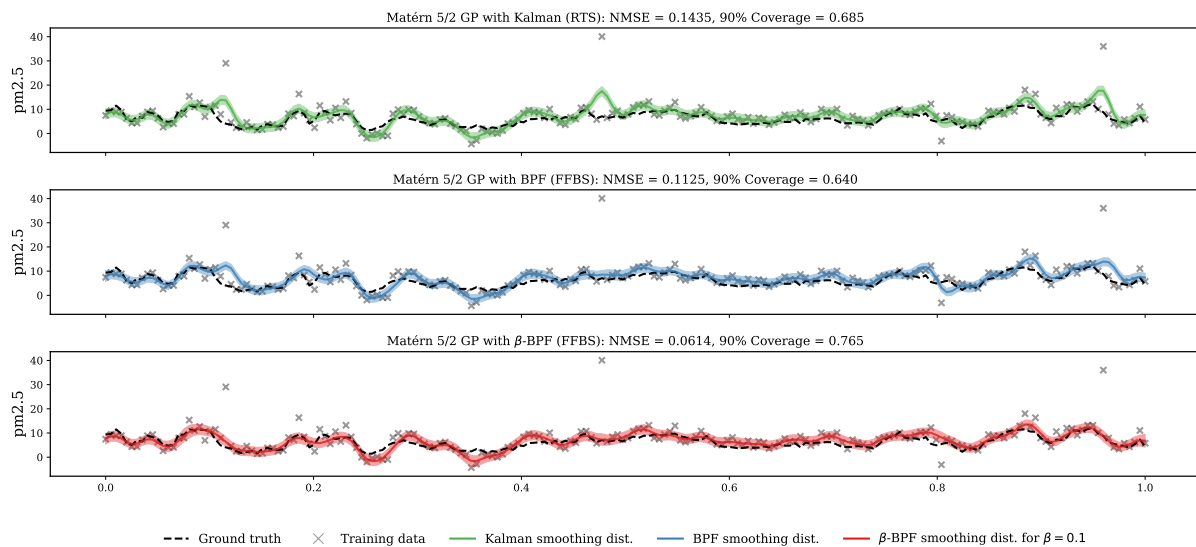


Figure 19: The GP fit on the measurement time series for one of the London air quality sensors. The top panel shows the posterior from the Kalman (RTS) smoothing. The middle panel shows the posterior from the BPF (FFBS). The bottom panel shows the posterior from the β -BPF (FFBS) for $\beta = 0.1$.